Chapter 5

Stability of Foams and Foam Films Containing Methyl Isobutyl Carbinol

Abstract

The thin film pressure balance (TFPB) technique was used to measure the equilibrium film thicknesses and disjoining pressure isotherms of foam films containing varying concentrations of a nonionic surfactant, Methyl Isobutyl Carbinol (MIBC), 4-methyl-2-pentanol, in the presence of $5x10^{-5}$ M NaCl. An attractive force (referred as hydrophobic force) was detected when surfactant concentration was below 10^{-5} M. The hydrophobic force appeared to be at least partially responsible for the high degree of instability of the foams and foam films at very low surfactant concentrations. The electrostatic double-layer repulsion decreased with increasing surfactant concentration, and played an important role in determining the stability of foams and foam films, in particular at high surfactant concentrations. In the middle surfactant concentration regime, however, the stability of three-dimensional foams can not be explained by the disjoining pressure of the corresponding foam films alone. However, the discrepancy can be attributed to the changes in film elasticity.

5.1 Introduction

Control of foam stability is of critical importance in many industrial applications such as tertiary oil recovery, froth flotation, food, and personal care products, etc. Foam is a dispersion of gas bubbles in a liquid. When the gas fraction is high, the bubbles contact with each other and deform, creating lamellae (thin film) and Plateau borders. The stability of foams is largely determined by the drainage and rupture of the thin films. The capillary pressure at the meniscus of a film serves as the driving force for the initial thinning of the film. When the film thickness is below 200 nm, the thinning process is controlled by surface forces. An attractive surface force tends to accelerate the film thinning process, and finally ruptures the film, therefore destabilizing the foam; a repulsive surface force tends to retard the film thinning process, leads to a final equilibrium state at a certain thickness, therefore stabilizing the foam. Therefore, it is very important to study surface forces in foam films for the sake of better understanding the factors affecting foam stability.

Derjaguin and Kussakov (1) represented the surface forces in terms of disjoining pressure, which is useful for describing the rupture process. The van der Waals force and electrostatic double-layer force are the two components of the disjoining pressure that form the basis of the Derjaguin-Landau-Verwey-Overbeek (DLVO) theory (2, 3). When two air bubbles interact with each other, the disjoining pressure due to the van der Waals forces is negative, while the disjoining pressure due to electrostatic double layer forces is positive. The disjoining pressure isotherm (the sum of the two forces as a function of separation distance) sheds light on the stability of thin aqueous films between air bubbles in contact.

Soap films exhibit a high degree of organization, and are therefore model systems in colloid and biological membrane science, in particular for the study of surface forces (4, 5). The DLVO theory is commonly used to explain the stability of foams and foam films with varying degrees of success. Discrepancies between DLVO theory and experiment were repeatedly found (6-9), indicating that the DLVO forces alone could not explain some experimental results. It is now generally recognized that non-DLVO forces such as steric force, hydration force and hydrophobic force are also important in determining the stability of thin films (10-15).

Air bubbles in water are hydrophobic, which is supported by recent sum frequency generation spectroscopy studies (16, 17). Hydrophobic interactions were observed widely in aqueous film between two macroscopic hydrophobic surfaces. It is established that there are hydrophobic interactions between two hydrophobic solid surfaces (18-25). The term “hydrophobic force” was first used by Blake and Kitchener (26) to explain the instability of wetting films which was considered to be due to attraction forces operating across the film which arise because of the contact of the water with the hydrophobic surfaces. Moreover, Bergeron (8) suggested that hydrophobic force might be responsible for the less stability of pseudo-emulsion films than corresponding foam films because the former is in a more hydrophobic environment. Bergeron (8) also reported a disjoining pressure isotherm at 10^{-3} M sodium dodecyl sulfate (SDS), which suggests the presence of an attractive force larger than the van der Waals forces. Therefore, hydrophobic force might play an important role in antifoaming and defoaming (27).

Recently, some thin film pressure balance (TFPB) studies suggested the presence of hydrophobic force in foam films (13, 14, 28, 29). It is now recognized that hydrophobic force decreases with increasing surfactant adsorption and ion binding on the film surfaces due to reduced area of bare hydrophobic air/water interface. Electrolyte effect on hydrophobic force in foam films was also observed when using ionic surfactant at low concentrations (13). The adsorption of the surfactant and its counterion made the system complex to evaluate the individual surface forces, in particular the electrostatic double-layer repulsion. Nevertheless, these results imply that there might be no single and simple mechanism behind the "hydrophobic attraction" in foam films at low electrolyte concentrations.

In this study, the hydrophobic force in foam films stabilized by a nonionic surfactant was studied using the TFPB technique. The basic idea of this paper is that the electrostatic forces are kept at a nearly constant magnitude, and the van der Waals forces are negligible for thick films or common black films in our case, whereas the hydrophobicity of air/water interfaces is changed so that the effects of hydrophobic force can be more readily evaluated. This can be achieved by using a weak nonionic surfactant at a low electrolyte concentration. The aim of this communication is to study the hydrophobic force in foam films stabilized by a nonionic surfactant, and evaluate its effects on the stability of the three-dimensional foams.

5.2 Materials and Methods

A Nanopure water treatment unit was used to obtain double-distilled and deionized water with a conductivity of 18.2 $M\Omega cm^{-1}$. Methyl Isobutyl Carbinol, MIBC (99%) from Research Chemicals Ltd. was used as received. A high-purity sodium chloride (99.99%) from Alfa Aesar was used as an electrolyte.

The TFPB technique developed by Scheludko and Exerowa (30) was used to measure the disjoining pressure in a single horizontal foam film. Basically, an optical technique, the microinterferometric technique (31) was used to measure the thickness of the film which is under a certain capillary pressure. The film thickness and capillary pressure are two important physical parameters to evaluate surface forces. The disjoining pressure isotherms were probed by measuring the equilibrium thickness of a film under varying gas pressure in a thermostated glass vessel, in which a film holder was placed. Two types of film holders were used. A Scheludko cell was used to measure equilibrium film thickness under low capillary pressure (i.e., below 75 Pa), which was controlled by changing the bulk surfactant concentration. The film radii were controlled below 0.15 mm, and the capillary pressure can be calculated using the following formula (32):

$$P_c = \frac{2\gamma}{R_c} \qquad [5.1]$$

where R_c(=2 mm) is the inner radius of the Sheludko cell. A bike-wheel microcell (33) with a hole diameter of 0.75 mm, was used to measure the disjoining pressure above 150 Pa, which was controlled by changing the bulk gas pressure in the glass vessel. The bike-wheel film holder is reusable, has a uniform liquid drainage inside, and exhibits an air/water entry pressure of about 10 KPa. The working equation for the measurement of disjoining pressure is (34),

$$\Pi = P_g - P_r + \frac{2\gamma}{r} - \Delta\rho g h_c \qquad [5.2]$$

where P_g is the pressure in the cell, P_r the external reference pressure, r the radius of the capillary tube connected with the film holder, $\Delta\rho$ the density difference between the aqueous solution and air, g the gravitational constant, and h_c is the height of aqueous column in the capillary tube above the film. The repeated measurement of h_c during the process of mapping out the entire disjoining pressure isotherm was bypassed by introducing a horizontal session of the capillary tube, along which the air/solution interface exposed to atmosphere moved horizontally within the controlled capillary pressure regime. The measuring error of disjoining pressure is less than 10 Pa.

The stability of three-dimensional foams was measured by the shake tests (35). The tests were conducted using 50 ml volumetric flasks filled with 25 ml of surfactant solution. Each solution was shaken by hand at fixed frequency and time, then left to stand. After a period of time, a clear water surface began to appear at the center of the foam. As the time elapses, the clear surface expanded toward the wall of the flask, forming a ring of bubbles, which subsequently broke into clusters of bubbles. The size of clusters was reduced with time, some of which eventually becoming isolated bubbles. For relatively stable foams, such as MIBC-stabilized foams in the presence of $5x10^{-5}$ M NaCl, the decay time of the foam was recorded as the time it took for a clear liquid surface to appear at the center of the foam and was denoted as τ^{I}. For relatively unstable foams, such as MIBC-stabilized foams in the presence of 0.1 M NaCl, the clear liquid surface at the center of the foam appeared immediately after the flask was shaken and left to stand. Therefore, the time it took until only the isolated bubbles became visible was taken as a measure of foam stability and was denoted as τ^{II}.

5.3 Results and Discussion

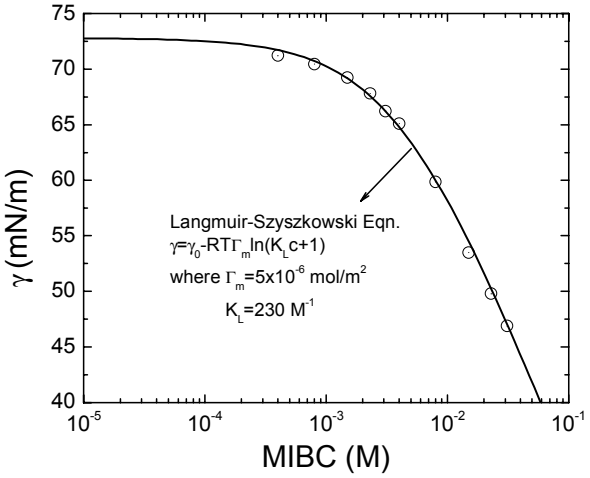

Figure 5.1 Static surface tension of MIBC solutions as a function of concentration (37).

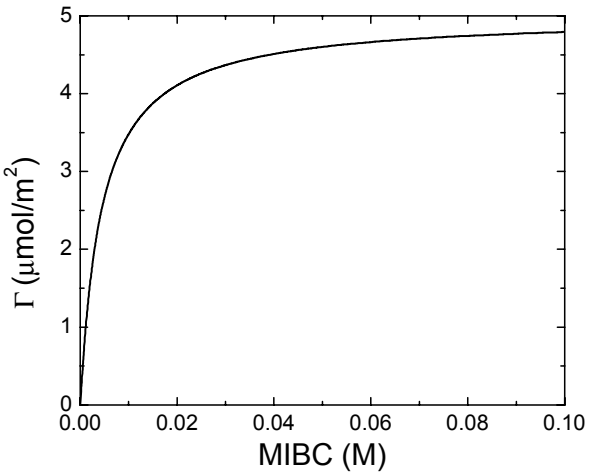

Figure 5.2 Surface excess for MIBC as a function of bulk concentration.

Figure 5.1 shows the static surface tension of MIBC solutions as a function of concentration, adapted from Comley et al. (36). Also plotted in the figure is the best fit of the Langmuir-Szyszkowski equation:

$$\gamma = \gamma_0 - RT\Gamma_m \ln(1 + K_L c) \qquad [5.3]$$

where γ_0 is the surface tension of pure water, Γ_m a maximum adsorption density, K_L the Langmuir equilibrium adsorption constant, and c the bulk concentration of MIBC. It gives $5\text{x}10^{-6}$ mol/m^2 for Γ_m, and 230 M^{-1} for K_L. The surface excess of MIBC at the air/water interface was then plotted in Figure 5.2 as a function of the bulk concentration using the Langmuir isotherm:

$$\Gamma = \frac{\Gamma_m K_L c}{1 + K_L c} \qquad [5.4]$$

Figure 5.3 shows the equilibrium film thickness (H_e) measured at varying MIBC concentrations in the presence of $5\text{x}10^{-5}$ M NaCl. Film rupture was observed when surfactant concentration was below 10^{-6} M or above 10^{-2} M. When increasing surfactant concentration from 10^{-5} M to 10^{-4} M, H_e decreased noticeably. This can be ascribed to the decrease in surface charge density at the film surfaces. Many authors argued that the presence of excess of OH^- ions should be the charge-determining ions, which cause the bare air/water interface to be negatively charged (37- 41). In the presence of competitive adsorption of nonionic surfactant molecules, some of the hydroxide ions may be expelled from the interface. However, the adsorbed neutral MIBC molecules themselves do not contribute to surface charge. On the whole, the more MIBC molecules adsorbed on the surface, the lower the surface charge density is. Therefore, the adsorption of MIBC tends to reduce the electrostatic repulsion.

Note, however, that H_e increased dramatically at higher surfactant concentrations (i.e., above 10^{-3} M). This may be caused by a rapid decrease in capillary pressure at the

meniscus of the Scheludko cell. It is well documented that the surface tension of MIBC starts to decrease noticeably above above 10^{-3} M. According to Eq. [5.1], the capillary pressure (P_c) on the films must also diminish with decrease in surface tension (γ).

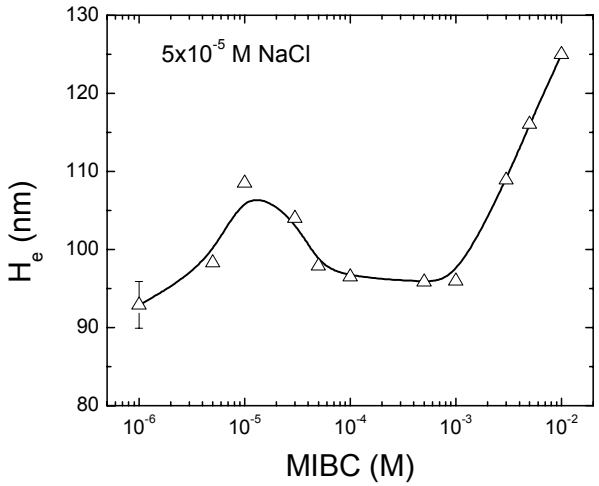

Figure 5.3 Equilibrium film thickness as a function of MIBC concentration in the presence of 5x10^{-5} M NaCl. The error bar is a typical one reflecting the repeatability of the measurements at the present ionic strength.

Interestingly, H_e increased considerably as MIBC concentration increased from 10^{-6} M to 10^{-5} M. Some investigators (39, 42) also observed an increase in film thickness with an increase in the concentration of a nonionic surfactant. A tentative explanation for their results may be a decrease in capillary pressure as they used strong surfactants, which are able to considerably decrease surface tension even at low bulk concentrations. In the present work, however, a much weaker surfactant (MIBC) was used. The surface tension remains nearly constant at the low MIBC concentrations. In this regard, the increase in equilibrium film thickness can not be ascribed to the changes of capillary pressure itself. It is therefore proposed that the changes in film thickness should be due to the changes of an additional non-DLVO force, hydrophobic force, associated with the change in MIBC concentration. It is likely that the surface potential at the air/water interface would remain constant at such low surfactant concentrations employed in the present work. Also, one can ignore the contributions from the van der Waals force at large film thicknesses.

The surface water molecule structure can be characterized by using the sum frequency generation (SFG) spectra, which find that the signature of the hydrophobicity of a surface may be the dangling free hydroxyl bonds. A recent SFG study (43) has shown that the peak of the free hydroxyl bonds starts to diminish when surfactant concentration is above 10^{-5} M, indicating that air/water interface is hydrophobic in the absence of surfactant molecules, and the interface becomes hydrophilic with increasing surfactant adsorption. Therefore, the high degree of surface hydrophobicity at MIBC concentrations below 10^{-5} M might give rise to hydrophobic force, which provides an explanation for the noticeable changes in equilibrium film thickness.

A series of disjoining pressure isotherms were measured in the present work at varying MIBC concentration in the presence of $5x10^{-5}$ M NaCl. Figure 5.4 shows a typical isotherm. Among all the isotherms, the disjoining pressure at 10^{-5} M MIBC was the highest, and reduced with either increasing or decreasing MIBC concentration. The decrease in disjoining pressure with increasing MIBC concentration correlates with a decrease in electrostatic double-layer repulsion. This, again, can be attributed to the displacement of hydroxide ions by surface excess of neutral MIBC molecules. Similar results were obtained by other investigators (35, 39). In the present work, the bike-wheel film holder has a minimum capillary pressure (about 150 Pa) exerting on a foam film, and as a result, no disjoining pressure isotherm was attainable above $3x10^{-3}$ M MIBC. This also helps justify our forgoing speculation that the remarkable increase in equilibrium film thickness at high surfactant concentrations, as shown in Figure 5.3, is due to the considerable decrease of surface tension, rather than the changes in disjoining pressure. The reduced disjoining pressure at high MIBC concentration can only predict film thickness lowering, which is in contradiction with the experimental results.

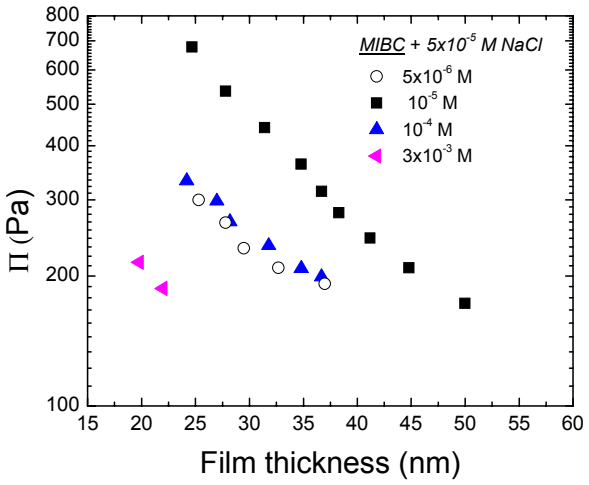

Figure 5.4 Disjoining pressure isotherm of MIBC at varying concentrations in the presence of $5x10^{-5}$ M NaCl.

It is interesting that in Figure 5.4 the measured disjoining pressure isotherm at $5x10^{-6}$ M MIBC is below the one at 10^{-5} M MIBC. This shows again that by evoking hydrophobic force in foam films at low surfactant concentrations we can explain the decrease in disjoining pressure measured at a MIBC concentration below 10^{-5} M. This phenomenon is in consistence with an increase in H_e as surfactant concentration increased from 10^{-6} M to 10^{-5} M (see Figure 5.3), where the double-layer repulsion and van der Waals attraction in the films and the capillary pressure are expected to change little. Note that $5x10^{-6}$ M is the lowest surfactant concentration where reliable disjoining pressure isotherm can be obtained in the present work.

Figure 5.5 shows the stability of three-dimensional foams measured by the shake tests. The time it took for a clear liquid surface to appear at the center of the foam was

recorded as τ^I. In the presence of 5x10^{-5} M NaCl, foam lifetime increased with increasing surfactant concentration, reached a maximum at 3x10^{-3} M, and then decreased with further increasing surfactant concentration. At either very low or very high surfactant concentrations the foams were unstable, which is consistent with the stability of individual films observed in the TFPB studies. Note, however, that the peak of foam lifetime curve in Figure 5.5 is at 3x10-3 M MIBC, quite different from where the highest disjoining pressure isotherm was obtained (10-5 M MIBC). It is hardly surprising as foam destruction is essentially a complex dynamic process subject to many influences. The surface forces measured in single films at equilibrium by themselves can not exactly account for all the factors affecting foam stability. This discrepancy can be explained somehow by the change of film elasticity, a "self-healing" capacity against external disturbance.

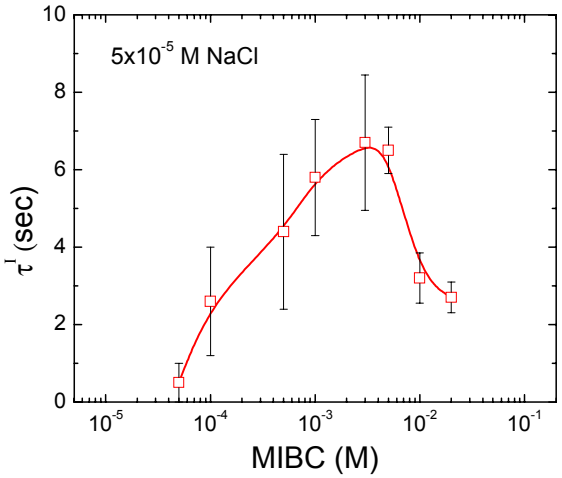

Figure 5.5 The lifetime of three-dimensional foams measured using shake tests as a function of MIBC concentration in the present of 5x10^{-5} M NaCl. The error bar denotes the maximum data scattering range.

The elasticity of foam films (E) is defined by Gibbs as follows:

$$E = 2A\frac{d\gamma}{dA} = 2A\frac{d\gamma}{dc}\frac{dc}{dA} \qquad [5.5]$$

where A is the film surface area, and c is the bulk surfactant concentration. For a closed system, the volume of a foam film, $V = AH$, is constant, *i.e.*, dV=0, where H is film thickness. Also, the total number of the surfactant molecules is constant. After several mathematical steps, including using the Gibbs adsorption isotherm, Wang and Yoon (44) derived an expression for E as follows:

$$E = \frac{4RT\Gamma^2}{c(H + 2d\Gamma/dc)} \qquad [5.6]$$

where Γ is the surface excess of a surfactant at an air/water interface. Equation [5.6] is similar to Christenson and Yaminsky's model (45), except that these authors ignored the

$d\Gamma/dc$ term, which is significant at low surfactant concentrations. Equation [5.6] can be transformed into a more useful form (44):

$$E = \frac{4RT\Gamma_m^{\,2}K_L^{\,2}c}{H(1+K_Lc)^2 + 2\Gamma_m K_L} \qquad [5.7]$$

by combining it with the Langmuir isotherm (see Eq. [5.4]). In Eq. [5.7], H was set equal to the measured H_e (except that H is set equal to 125 nm at MIBC concentrations above $3x10^{-2}$ M), and the Γ_m and K_L values were set equal to those determined from the best fit of the Langmuir-Szyszkowski equation (Eq.[5.3]) to the surface tension data shown in Figure 5.1.

Note that the plot of E versus c exhibits a maximum at $3x10^{-2}$ M MIBC, which is also different from the peak of foam lifetime shown in Figure 5.5. The peak in Figure 5.6 can be attributed to the competition of two effects: (i) surfactant adsorption at low surfactant concentrations, and (ii) molecular exchange at high surfactant concentrations (46). These two effects are implicitly reflected in Eq. [5.6] by Γ and $d\Gamma/dc$, respectively.

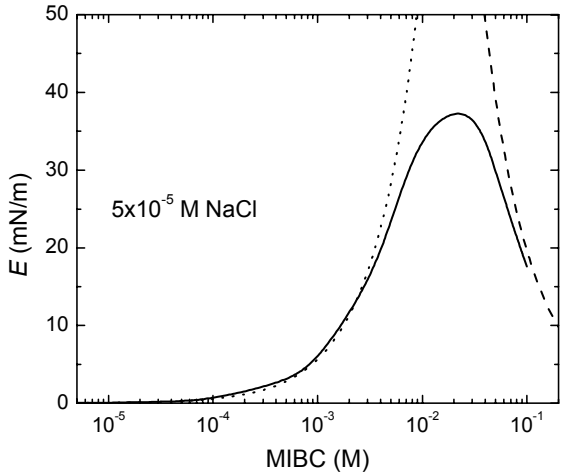

Figure 5.6 Effect of MIBC concentration on film elasticity (E). Film elasticity was calculated using Eq. [5.7], where Γ_m and K_L were determined from the best fit of the Langmuir-Szyszkowski equation (Eq. [5.3]) to the surface tension data shown in Figure 5.1, and H_e values were those plotted in Figure 5.3 (expect above $3x10^{-2}$ M MIBC where H_e was set equal to 125 nm). Equation [5.7] can be approximated by Eq. [5.8] (dotted line) at low MIBC concentrations and Eq. [5.9] (dashed line) at high MIBC concentrations.

At very low MIBC concentrations, one can expect that $H(1+K_Lc)^2 << 2\Gamma_m K_L$, so Eq. [5.7] can be approximated by

$$E = 2RT\Gamma_m K_L c \qquad [5.8]$$

which is equivalent to the most commonly used formula, $E_G = -2\Gamma d\gamma/d\Gamma$, based on the assumption that no molecular exchange occurs between the interface and the bulk.

Equation [5.8] was plotted in Figure 5.6 as a dotted line. As shown, E increases monotonically with increasing MIBC concentration at low concentration region.

At MIBC concentrations above $3x10^{-2}$ M, which is expect to approach the critical micellization concentration (CMC), one can see that $\Gamma \rightarrow \Gamma_m$, and $d\Gamma/dc \rightarrow 0$, Eq. [5.7] can be approximated by

$$E = \frac{4RT\Gamma_m^{\ 2}}{cH} \qquad [5.9]$$

from which E was found to be proportional to $1/c$ if H is set to be a fixed value. Equation [5.9] was plotted in Figure 5.6 as a dashed line with H being set as 125 nm. The line essentially acts as a limit of E at high MIBC concentrations around the critical micellization concentration (CMC). The sharp decrease in E as MIBC concentration is approaching to its CMC shows that Eq. [5.7] can be applied to explain the sharp peak of the foam stability in systems approaching the CMC of the surfactant. The advantage of Eq. [5.7] is, however, that all the parameters required can be readily obtained from the measurement of film thickness (H) and the fit of surface tension data using Eq. [5.3] for Γ_m and K_L values.

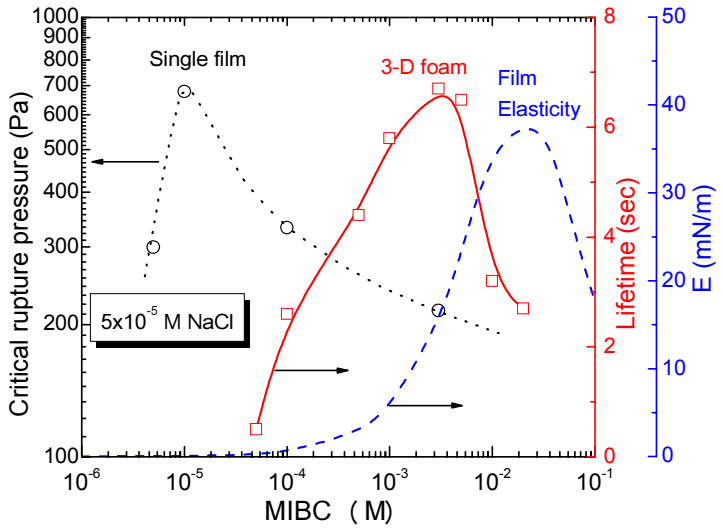

Figure 5.7 The effects of MIBC concentration on the critical rupture pressure of single films (taken from Figure 5.4), lifetime of three-dimensional foams (taken from Figure 5.5), and film elasticity (E) (taken from Figure 5.6).

The stability of a single foam film can be characterized by the positive barrier height of its disjoining pressure isotherm (i.e., the critical rupture pressure). In the present work, critical rupture pressures were only attainable at surfactant concentrations from $5x10^{-6}$ M to $3x10^{-3}$ M, and were plotted in Figure 5.7. The stability of foams was replotted here for comparison. The critical rupture pressure first increased from 300 Pa at $5x10^{-6}$ M to 678 Pa at 10^{-5} M, reaching a maximum, and then decreased to 332 Pa at 10^{-4} M and 215 Pa at $3x10^{-3}$ M, respectively. The most stable films were at 10^{-5} M MIBC. On

the other hand, the maximum film elasticity was at $3x10^{-2}$ M MIBC. Between these two finds $3x10^{-3}$ M MIBC, where the most stable foam was obtained. This implies that foam stability at MIBC concentrations between 10^{-5} and $3x10^{-2}$ M may be jointly determined by disjoining pressure and film elasticity.

Further, the stabilities of MIBC-stabilized foams are compared at distinct electrolyte concentrations and are shown in Figure 5.8. The lifetime for the former was recorded as τ^{I} and the lifetime for the latter was recorded as τ^{II}. These curves were deployed purposely to show that foams in the presence of $5x10^{-5}$ M NaCl were much more stable than in the presence of 0.1 M NaCl. τ^{I} increased with increasing MIBC concentration, reaching a maximum at $3x10^{-3}$ M before decreasing at higher concentrations. On the other hand, τ^{II} monotonically increases with increasing MIBC concentration. Obviously, this distinction can not be simply attributed to the change in film elasticity in that the surface tension isotherm of MIBC, as a nonionic surfactant, is not sensitive to adding NaCl. The decrease in the stability of foams at MIBC concentrations above $3x10^{-3}$ M in the presence of $5x10^{-5}$ M NaCl is most likely due to the decrease in double-layer repulsion caused by the decrease in surface charge density at high concentrations of a nonionic surfactant (35, 39, 40). At 0.1 M NaCl, the absence of double layer force allows film elasticity to play a more important role in stabilizing the foams at moderate and high surfactant concentrations.

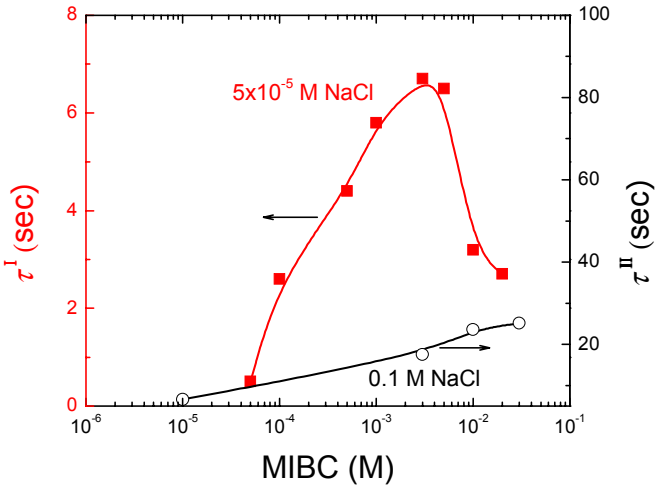

Figure 5.8 Effects of MIBC concentration on the stability of foams measured by the shake tests: (■), τ^{I}, the time it took for the appearance of liquid surface for foams in the presence of $5x10^{-5}$ M NaCl; (○), τ^{II}, the time it took until only the isolated bubbles became visible for foams in the presence of 0.1 M NaCl.

5.4 Conclusions

The thin film balance (TFPB) technique was used to measure the equilibrium thicknesses and disjoining pressure isotherms of foam films containing MIBC in the presence of $5x10^{-5}$ M NaCl. The results qualitatively showed the presence of hydrophobic

force at very low MIBC concentrations. The stabilities of the foam films were compared to the foam stabilities measured using the shake tests and the film elasticities calculated from surface tension. The results showed that one could control foam stability by balancing the elasticities and the disjoining pressure of the foam films.

5.5 References

1. Derjaguin, BV; Kussakov, M.M., *Acta Phys. Chim*. URSS. 10 (1939) 25.
2. Derjaguin, B.V. and Landau, L., *Acta Physicochim. U.R.S.S.* 14 (1941) 633.
3. Verwey, E.J.W. and Overbeek, J.T.G., *Theory of the Stability of Lyophobic Colloids*, Elsevier, Amsterdam, 1948.
4. Bélorgey O. and Benattar, J.J., *Physical Review Letters*, 66 (1991) 313.
5. Sentenac D. and Dean, D.S., *J. Colloid Interface Sci*., 196 (1997) 35.
6. Lyklema, J. and Mysels, K.J., *J. Amer. Chem. Soc*., 87 (1965) 2539.
7. Exerowa, D., Kolarov, T. and Khristov, Khr., *Colloids and Surfaces*, 22 (1987) 171.
8. Bergeron, V., Ph.D. thesis, University of California at Berkeley, 1993.
9. Tchaliovska, S, Manev, E, Radoev, B, Eriksson, J C, and Claesson, P M, *J Colloid Interface Sci,* 168 (1994) 190.
10. Sedev, R., Németh Zs., Ivanova R., Exerowa, D., *Colloids Surfaces A: Physicochem. Eng. Aspects.* 149 (1999) 141.
11. Ruckenstein, E., and Bhakta, A., *Langmuir*, 12 (1996) 4134-4144.
12. Bergeron, V., *J. Phys., Condensed Matter*, 11 (1999) R215.
13. Wang, L, and Yoon, R –H, *Langmuir*, 20 (2004) 11457.
14. Angarska, J. K., Dimitrova, B. S., Danov, K. D. Kralchevsky, P. A., Ananthapadmanabhan, K. P., and Lips, A., *Langmuir,* 20 (2004) 1799.
15. Churaev, N.V., *Advances in Colloid and Interface Sci.*, 114–115 (2005) 3-7.
16. Du, Q., Superfine, R., Freysz, E. and Shen, Y.R., *Phys. Rev. Lett*. 70 (1993) 2313.
17. Du, Q., Freysz, E. and Shen, Y.R., *Science*, 264 (1994) 826.
18. Israelachvili, J.N. and Pashley, R. *Nature*, 300 (1982) 341-342.
19. Israelachvili, J.N. and Pashley, R.M., *J. Colloid Interface Sci*. 98 (1984) 500.
20. Pashley, R.M., McGuiggan, P.M., Ninham, B.W., Evans, D.F., *Science* 229 (1985) 1088.
21. Christenson H.K.,; Claesson, P.M. *Science* 239 (1988) 390.
22. Rabinovich, Y.I.; Yoon, R.-H. *Colloids Surf. A* 93 (1994) 263.
23. Lin, Q., Meyer, E.E., Tadmor, M., Israelachvili, J. N. And Kuhl, T., *Langmuir*, 21 (2005) 251.
24. Meyer, E.E., Liu, Q., and Israelachvili, J.N., *Langmuir*, 21 (2005) 256-259.

25. Zhang, J., Yoon, R.-H., Mao, M. and Ducker, W.A., *Langmuir*, 21 (2005) 5831.

26. Blake, T. D.; Kitchener, J. A., *J. Chem. Soc. Faraday Trans*. 68 (1972) 1435.

27. Denkov, N.D., *Langmuir*, 20 (2004) 9463.

28. Yoon, R. –H., and Aksoy B. S., *J Colloid Interface Sci,* 211 (1999) 1.

29. Wang, L., and Yoon, R.–H., *Colloids Surfaces A: Physicochem. Eng. Aspects*, 263 (2005) 267.

30. Scheludko, A. and Exerowa, D., *Comm. Dept. Chem., Bul. Acad. Sci.*, 7 (1959) 123.

31. Scheludko, A. Thin liquid films. *Advances in Colloid and Interface Sci*. 1 (1967) 391.

32. Exerowa, D. and Kruglyakov, P. M., *Foam and Foam Films*, Elsevier, 1998.

33. Cascão Pereira, L. G., Johansson, C., Blanch, H. W. and Radke, C. J., *Colloids and Surfaces A: Physicochem Eng Aspects,* 186 (2001) 103.

34. Bergeron V.; Radke, C.J. *Langmuir* 8 (1992) 3020.

35. Waltermo, Å, Claesson, P M, Simonsson, S, Manev, E, Johansson, I, Bergeron, V., *Langmuir,* 12 (1996) 5271.

36. Comley, B.A., Harris, P.J., Bradshaw, D.J., Harris, M.C., *Int. J. Miner. Process*. 64 (2002) 81.

37. Yoon R. –H., and Yordan, J. L., *J Colloid Interface Sci,* 113 (1986) 430.

38. Manev, E, and Pugh, R J, *Langmuir,* 7 (1992) 2253.

39. Bergeron, V, Watermo, Å, and Claesson, P M, *Langmuir,* 12 (1996) 1336.

40. Karraker, K A, and Radke, C J, *Advances in Colloid and Interface Sci,* 96 (2002) 231.

41. Stubenrauch, C, and Klitzing, R, *Journal of Physics: Condensed Matter,* 15 (2003) R1197.

42. Exerowa, D., Zacharieva, M, Cohen, R, and Platikanov, D., *Colloid and Polymer Sci,* 257 (1979) 1089.

43. Kumpulainen, A.J., Persson, C.M., Eriksson, J.C., Tyrode, E.C., Johnson, C.M., *Langmuir* 21 (2005) 305.

44. Wang, L. and Yoon, R.-H, *Colloids Surfaces A: Physicochem. Eng. Aspects*, in press.

45. Christenson H.K. and Yaminsky, V. V., *J. Phys. Chem.* 99 (1995) 10420

46. Stubenrauch, C., Miller, R., *J. Phys. Chem. B* 108 (2004) 6412.